INTERNATIONAL ATOMIC ENERGY AGENCY
UNITED NATIONS EDUCATIONAL, SCIENTIFIC AND CULTURAL ORGANIZATION
INTERNATIONAL CENTRE FOR THEORETICAL PHYSICS
I.C.T.P., P.O. BOX 586, 34100 TRIESTE, ITALY, CABLE: CENTRATOM TRIESTE

H4.SMR/449-19

WINTER COLLEGE ON HIGH RESOLUTION SPECTROSCOPY

(8 January - 2 February 1990)

CAVITY QUANTUM ELECTRODYNAMICS: RYDBERG ATOMS IN ATOMIC PHYSICS & QUANTUM OPTICS

H. Walther
& G. Rempe

Sektion Physik
Universität München &
Max-Planck-Institut für Quantenoptik
D-8046 Garching
F.R. Germany

CAVITY QUANTUM ELECTRODYNAMICS: RYDBERG ATOMS IN ATOMIC PHYSICS AND QUANTUM OPTICS

G. Rempe and H. Walther
Sektion Physik, Universität München,
and Max-Planck-Institut für Quantenoptik
D-8046 Garching, F.R. Germany

ABSTRACT. The progress achieved during the last years in using Rydberg atoms to investigate radiation-atom interaction is reviewed. In particular, the influence of blackbody radiation, the modification of the spontaneous emission rate in confined space, and the periodic exchange of photons between Rydberg atoms and a cavity field are discussed. In the latter case, the collapse and the revival in the dynamical behaviour of the atoms are observed. Furthermore, the generation of nonclassical radiation fields in the micromaser is addressed.

1. Introduction

The advent of the laser, and even more the development of frequency-tunable lasers have revolutionized spectroscopy. An outstanding example of the new possibilities is the spectroscopy of highly excited atomic states, the so-called Rydberg states or Rydberg atoms. These are atoms with a valence electron excited into an orbit of very high principal quantum number, i.e. far from the ionic core. The energies of these highly excited levels are well described by the Rydberg formula, because of their hydrogenic nature. The existence of hydrogen Rydberg atoms has been known from radio astronomy for many years. In space, they are produced when protons capture electrons in high orbits; radio waves are then emitted when the electron jumps to lower energy levels. Until recently, however, it was impossible to investigate Rydberg atoms in the laboratory. In particular, it is not possible to populate highly excited states in discharges, since their large collisional cross-section prevents their formation. It was the availability of tunable lasers of sufficient intensity and narrow bandwidth that first made the selective excitation of these states possible. An excellent review on the properties of Rydberg atoms is given in the book of Stebbings and Dunning [1].

Owing to their high principal quantum numbers, and also to the small energy difference between neighbouring levels, Rydberg atoms exhibit a number of classical properties. In particular, according to Bohr's correspondence principle, the transition frequency between neighbouring levels approaches the classical evolution frequency of the electron. On the other hand, these systems also represent an almost ideal testing

ground for some of the most fundamental models and predictions of low energy quantum electrodynamics (QED). The reasons are the following:

(a) The dipole interaction between electromagnetic radiation and Rydberg atoms is very large, the corresponding matrix elements between neighbouring levels scale as n^2 (n is the principal quantum number). For high enough n, stimulated effects can overcome spontaneous emission even for fields with very small photon numbers. As a consequence, Rydberg atoms are very sensitive, e.g. to blackbody radiation [2-8].

(b) Because of the large wavelength of the radiation emitted in Rydberg transitions, it is possible to modify the radiative properties of the atoms by modifying the boundaries of the space in which the atoms are contained [9-19]. The consequences are the enhancement or inhibition of the rate of spontaneous emission, depending upon an external cavity being tuned on or off resonance with a transition frequency. The Lamb shift can be modified as well in such experiments [20-22].

(c) For cavities with high quality factors, the photon emitted by a Rydberg atom is stored inside the resonator long enough to be reabsorbed. In this way, it is possible to realize a single-atom maser [23-24].

(d) A single Rydberg atom inside a low-loss single-mode resonator is the experimental version of the Jaynes-Cummings model [25], which describes the interaction between a single two level atom and a single mode of the electromagnetic field. This model has been the subject of considerable attention in the past, and a number of purely quantum mechanical predictions on the dynamics of this system have been made. These include the collapse and the revivals in the dynamics of the atomic population [26-34]. Rydberg atoms for the first time offer a possibility to test these predictions.

(e) The field generated inside the cavity of the single-atom maser shows nonclassical properties [35-40]. The photon number distribution is narrower than a Poissonian distribution. Theory predicts, that under suitable conditions even a number state of the electromagnetic field can be generated [37-38]. This purely quantum mechanical state has no intensity fluctuations. The one-atom maser can therefore be used to study for the first time the interaction of atoms with a light field with fluctuations below the shot noise limit.

The rest of this paper is organized as follows. In section 2, we briefly review some important properties of Rydberg atoms. Section 3 discusses the influence of blackbody radiation on their dynamics, and section 4 shows how the rate of spontaneous emission is modified by placing the atom in an appropriate environment. In section 5, we turn to a brief discussion of the one-atom maser, while section 6 recalls some results of the quantum-mechanical Jaynes-Cummings model. Section 7 discusses the experimental observation of collapse and revival of the oscillatory energy exchange between the atom and the field. Section 8 reviews the most important properties of the field generated by the one-atom maser. Finally, section 9 contains a summary and conclusions.

2. Properties of Rydberg atoms

When a valence electron of an atom is excited into a state of high principle quantum number n, the energy of the atom can be described by the

Rydberg formula with n replaced by an effective principle quantum number n^*. In general, n^* depends on the phenomenological quantum defect δ_l of the state of angular momentum l. For low-l states, where the orbits of the classical Bohr-Sommerfeld theory are ellipses of high eccentricity, the penetration and polarization of the electron core by the valence electron lead to large quantum defects and strong departures from hydrogenic behaviour. As l increases, the orbits become more circular and the atom more hydrogenic; as a result, δ_l decreases. The radius of the Rydberg atom scales as n^{*2}. Rydberg atoms therefore are very sensitive to external electric fields. As a consequence, they ionize in rather weak fields. This opens the possibility of very effective detection.

The large Rydberg atom orbitals are characterized by natural lifetimes much longer than those of less excited atoms. The lifetimes scale as n^{*3} (l small) or as n^{*5} (l large). The rate of spontaneous emission for a transition from state n to n′ is given by the Einstein coefficient

$$A_{nn'} = 16\pi^3\nu^3e^2\langle r_{nn'}\rangle^2/3\epsilon_0hc^3,$$

where ν is the transition frequency and $\langle r_{nn'}\rangle$ the matrix element of the electric dipole operator between the initial state n and final state n′. For the case $n'\ll n$, $\langle r_{nn'}\rangle$ is small, owing to the small radial overlap of the wavefunctions for n′ and n, and $A_{nn'}\propto n^{*-3}$ and n^{*-5} for small and large l, respectively. If $n'\approx n$, the energy difference $E_n-E_{n'}\propto n^{*-3}$ and $\langle r_{nn'}\rangle^2\propto n^{*4}$, so that $A_{nn'}$ becomes proportional to n^{*-5}. Since the matrix element $\langle r_{nn'}\rangle$ ($n\approx n'$) scales as n^{*2}, this leads to rather high induced transition probabilities. Rydberg atoms therefore strongly absorb microwave radiation. As a consequence, blackbody radiation emitted e.g. by the walls of the vacuum chamber may cause strong mixing of the states.

3. Influence of blackbody radiation on Rydberg atoms

We now turn to a discussion of the scaling laws related to these blackbody induced effects. The induced transition rate due to blackbody radiation is proportional to $\langle r_{nn'}\rangle^2S_\nu$, where S_ν is the energy flux of blackbody radiation per unit bandwidth and unit surface area. At low frequencies (Rayleigh-Jeans limit) S_ν increases as ν^2. As the distance between the Rydberg states scales as n^{-3} (for simplicity, we will use n instead of n^* for the following discussion), S_ν is proportional to n^{-6}. Since $\langle r_{nn'}\rangle^2\propto n^4$, the induced transition rate scales as n^{-2}. Important in experiments is the ratio between induced and spontaneous transition rates, which scales with $n^{-2}/n^{-3}=n$ for small l, and n^3 for large l. This means that for a given atom and a given temperature, there exists an n above which the blackbody-induced rate overcomes spontaneous emission.

Blackbody radiation mainly induces transitions to nearby states. As a result the population will evolve as a function of time after pulsed laser excitation. Changes in the populations typically appear on a microsecond time scale. Experiments were done using field ionization of Rydberg atoms with an electric field pulse rising linearly in time. Since various Rydberg states ionize at different electric field strengths, the population distribution among Rydberg states can be measured in a single shot. We measured this population distribution for

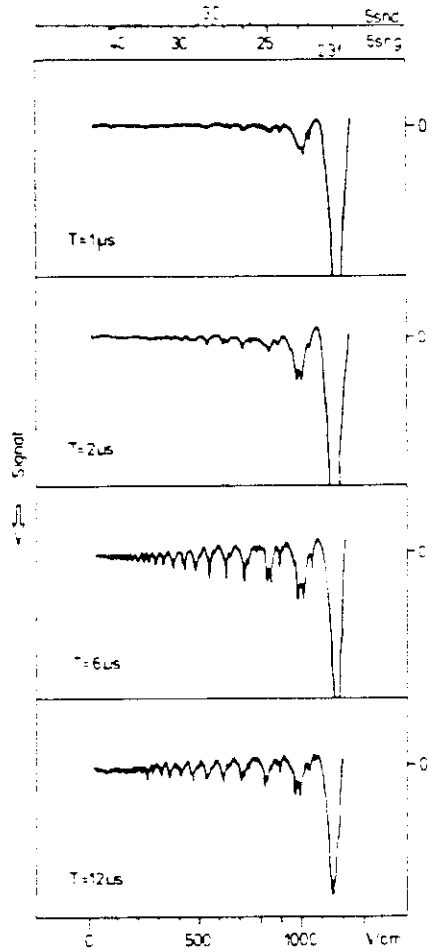

Fig.1: Blackbody-induced transitions between Rydberg states of Sr. The 23f level is excited by pulsed laser radiation. The detection of the Rydberg states is performed by an electric field increasing linearly in time and starting 1, 2, 6, and 12μs after the laser excitation. The field ionization signal at smaller field strengths results from Rydberg levels populated by blackbody radiation originating from the walls of the vacuum chamber at 300K.

various time delays between the pulsed laser excitation and the ionizing electric field pulse. It was observed that for increasing delay the population initially prepared in a Rydberg state was transferred to higher-lying states (fig.1). In these experiments, the temperature of the walls of the vacuum chamber was 300K [6].

Direct observations of the temperature dependence of the population transfer were performed in [7], where sodium atoms of a thermal beam in a cooled environment were excited to the 22d state using two continuous wave dye lasers. The interaction region was cooled to 14K. In another experiment on rubidium Rydberg atoms the environment was cooled to liquid helium temperature [8]. Fig.2 shows the experimental set-up. Two Rb atomic beams were excited stepwise by the light of three semiconductor diode lasers. The atomic beam on the left-hand side of

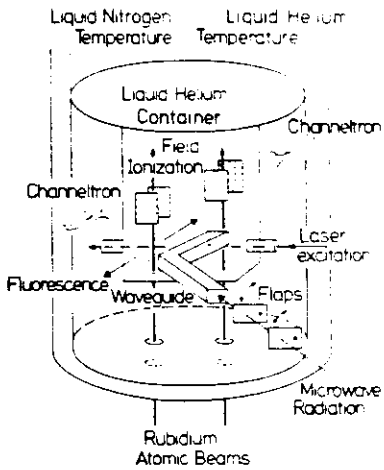

Fig.2: Experimental set-up of the 'Rydberg detector'. The two atomic beams are shielded with liquid nitrogen and liquid helium cooled surfaces. The left atomic beam is used to stabilize the frequency of the diode lasers; the right beam is used to detect microwave radiation.

fig.2 was used to stabilize the frequency of the diode lasers. Lasers 1 and 2 were stabilized using the fluorescence of the beam, whereas laser 3, which populated the Rydberg level, was stabilized by means of the signal current produced in the field ionization region.

The Rb beam on the right-hand side of fig.2 was used to study the interaction with the blackbody radiation. Fig.3 shows the signal obtained in the field ionization region of this beam when the $40P_{3/2}$ level was populated. The blackbody radiation populates the higher levels as indicated by the arrows on the left-hand side of fig.3. The strongest contribution results from the 181 GHz transition. The p-d transitions have a transition probability 100 times smaller than p-s transitions.

Changing the field strength of the ionizing field allowed the population of either the $43S_{1/2}$ or $42S_{1/2}$ level to be monitored. The contribution of the 40D and 41D levels can be neglected. The two signals are shown on the right-hand side of fig.3, as the upper and lower trace, respectively. Since the induced transition rate of the $40P_{3/2}$-$42P_{1/2}$ transition is about a factor of two larger than that of $40P_{3/2}$-$43S_{1/2}$, the field ionization signal of the $42S_{1/2}$ is correspondingly larger. The signals on the right-hand side of fig. 3 were obtained from 77K and 300K blackbody radiation, respectively. In the first case, it was emitted by the walls of the liquid nitrogen-cooled surface, and injected into the apparatus through the waveguide shown in fig. 2 (with the liquid helium-cooled flap open), while in the second case both flaps were open and the radiation was due to the 300K walls of the vacuum chamber. When comparing the results, it is of course important to take into account the different solid angles in each situation.

The evaluation of the data of fig.3 leads to a noise equivalent power of the 'Rydberg detector' of $10^{-17}WHz^{-1/2}$, a value comparable to the result of our earlier experiment [7]. But this new set-up clearly demonstrates that semiconductor lasers can be used to populate the Rydberg levels, making the Rydberg detector a more practical device.

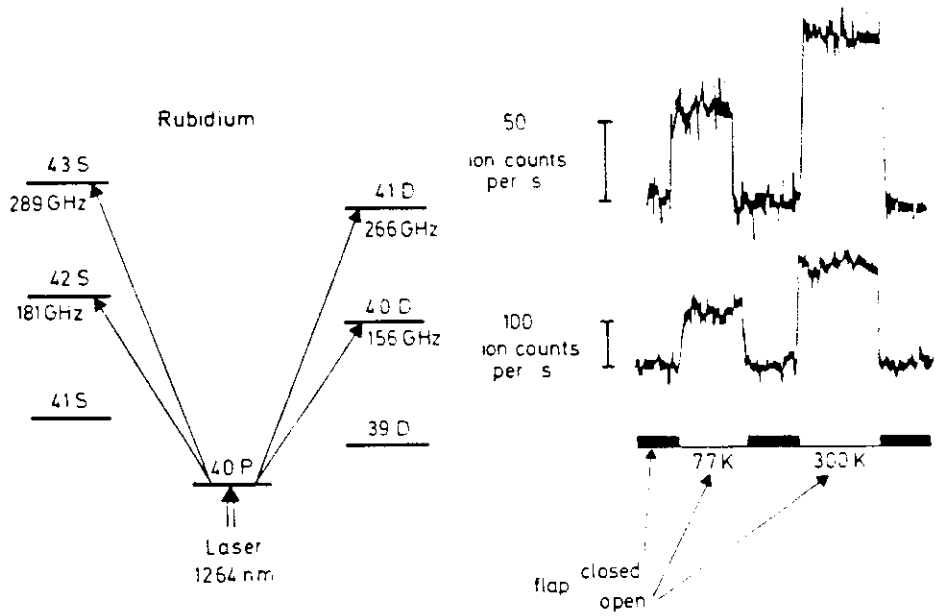

Fig.3: Left: Rubidium Rydberg states relevant for the experiment. The $40P_{3/2}$-$42S_{1/2}$ transition has the highest transition probability. Right: Field ionization signal of the $43S_{1/2}$ level (upper trace) and the $42S_{1/2}$ level (lower trace), respectively.

Aside from population transfer, blackbody radiation also affects Rydberg atoms in a more subtle way. The spectral energy density distribution of thermal radiation at 300K has its maximum at about $2 \cdot 10^{13}$Hz. This is to be compared to a typical electric dipole transition starting from an atomic ground state, which has a frequency of 10^{14}-10^{15}Hz and a transition between two Rydberg states, at about 10^{11}Hz. The blackbody radiation thus appears as a slowly varying field to a ground-state atom, and as a rapidly varying one to a Rydberg atom. This leads to a dynamic Stark shift of the Rydberg levels. An accurate evaluation of this shift was performed by Farley and Wing [41], who found that all Rydberg states experience roughly the same energy shift of about 2.4kHz at 300K.

Since the shift induced by blackbody radiation is roughly the same for all Rydberg states, it can be detected only as a change of frequency of the optical transition to the ground state. The extremely small shift was measured using Doppler-free two-photon absorption to excite the 5s-36s transition in rubidium atoms [42]. With the Ramsey method of separated fields, the spectral width of the signal at $5 \cdot 10^{14}$Hz was decreased to 40kHz. The line centre could be determined with an accuracy of 150Hz. When the temperature of the blackbody source was raised to about 500K, a shift in the line position of 1.4kHz was observed. The study of the temperature dependence also showed agreement with the predicted T^2 scaling. As pointed out in [43], the absolute temperature of the environment can be determined by measuring the blackbody-induced level shift.

4. Single atom in a cavity - modification of the spontaneous lifetime

It is well-known that the spontaneous lifetime of an excited atom is proportional to the density of modes of the electromagnetic field $\rho(\omega_k)$ about the atomic transition frequency ω_0 [44]. The spontaneous emission rate for a two-level system is increased if the atom is surrounded by a cavity tuned to the transition frequency. This was noted years ago by Purcell [9]. Conversely, the decay rate decreases when the cavity is mistuned [12]. In the case of an ideal cavity far off the atomic resonance, no mode is available to accept the emitted photon. As a consequence, spontaneous emission cannot occur. In the following, we would like to discuss this phenomenon in more detail.

Consider a cubic cavity of length L and quality factor Q. Owing to the finite Q, the cavity exhibits some losses which yield a cavity linewidth $\delta\omega=\omega/Q$. For a Lorentzian lineshape, the density of modes around a cavity mode of frequency ω_c and mode volume V_c is given by

$$\rho_c(\omega) = (1/2\pi V_c Q)\cdot[\omega_c/((\omega-\omega_c)^2+(\omega_c/2Q)^2)] \ .$$

At resonance $\omega_0=\omega_c$, this gives

$$\Gamma_c = \Gamma_f(Q/4\pi^2)(\lambda^3/V_c)$$

where Γ_c and Γ_f are the spontaneous emission rates in the resonator and in free space, respectively.

From this equation, we draw two important conclusions. At optical frequencies, the size of the resonator is large compared to the wavelength, resulting in a small ratio λ^3/V. However, for cavities operating near their fundamental frequencies in the microwave region, the ratio $\lambda^3/V_c\approx 1$, which typically results in high enhancements in the case of high Q resonators. We conclude that when an atom is placed inside a cavity with a single mode at its transition frequency, it radiates about Q/π^2 faster than in free space. This enhancement of the radiation rate was first pointed out by Bloembergen and Pound [45] and is the rational for using resonant cavities in lasers and masers.

Since a resonant cavity enhances spontaneous emission, it is not surprising that a nonresonant cavity depresses it. Consider for instance a cavity whose fundamental frequency is at twice the resonant frequency of the atomic transition. In this case, the radiation rate becomes

$$\Gamma_c = \Gamma_f\rho_c(\omega_0=2\omega)/\rho_f(\omega) = \Gamma_f/4\pi^2 Q \ .$$

Γ_c can be made arbitrarily small by making Q sufficiently large.

It is clear that cavity effects will in general also influence the Lamb shift of energy eigenstates. Since the Lamb shift itself is already fairly small for highly excited states, the expected changes turn out to be extremely small [20-22].

To demonstrate experimentally the modification of the spontaneous decay rate, it is not always necessary to use single atoms. The experiments where the spontaneous emission is inhibited can also be performed with higher densities. However, in the opposite case where an

increase of the spontaneous rate is observed, a large number of excited atoms increases the field strength in the cavity and the induced transitions disturb the experiment.

The first experimental work on inhibited spontaneous emission is due to Drexhage, Kuhn and Schäfer performed in 1974 [10]. They studied the fluorescence of a dye film on a mirror and observed an alteration of the fluorescence lifetime arising from the interference of the molecular radiation with its surface image.

Inhibited spontaneous emission was observed clearly for the first time by Gabrielse and Dehmelt [13]. They studied a single electron stored in a Penning trap and observed that the cyclotron excitation showed a lifetime up to ten times larger than that calculated for a cyclotron orbit in free space. The electrodes of the trap form a cavity which decouples the cyclotron motion from the vacuum radiation field.

Recently, an experiment with Rydberg atoms was performed [14]. When the atom was placed between two parallel conducting plates a change in the absorption of infrared radiation was observed. A similar set-up was used to demonstrate inhibited spontaneous emission [15]. The atoms used in this experiment were excited to a circular orbit with $n=22$ and angular momentum quantum number $l=21, |m_l|=21$. The only decay channel to the state with $n=21, l=20, |m_l|=20$ was partly suppressed by the plates. This led to a longer lifetime of the excited state by a factor of 20.

Recently, experiments were done with low-lying atomic states as well. A 13-fold increase of the lifetime of the low-lying 5d state of Cesium atoms between plates separated by only one micrometer could be demonstrated [16]. In addition, shifts in the frequency of the resonance transition of Barium atoms in an optical resonator, due to radiative effects, and changes in the linewidth, due to enhanced and suppressed spontaneous emission were observed [17]. The change of the fluorescence lifetime under short-pulse laser excitation of dye molecules in a microscopic cavity was also observed [18].

The first observation of enhanced atomic spontaneous emission in a resonant cavity was published by Goy, Raimond, Gross and Haroche [19]. Their experiment was performed with Rydberg atoms of Na excited to the 23s state in a niobium superconducting cavity resonant at 340GHz. A shortening of the lifetime was observed taking advantage of the high Q value of the superconducting resonator. The cooling necessary for superconducting operation also had the advantage of totally suppressing the blackbody field contributions, a necessary requirement to test purely spontaneous emission effects in the cavity.

In spite of this enhancement of spontaneous emission, the cavity damping rate of the radiation was still much higher. The probability of reabsorbing the emitted photon either by the same atom, or by a new atom entering the cavity, could be neglected. Further improvements of the cavity Q lead to a regime where these effects become important. This allows in particular the experimental realization of a single-atom maser [23-24] and for the first time provides experimental conditions close to those required to test the Jaynes-Cummings model [25], which describes the simplest and at the same time most fundamental interaction between a single radiation field mode and a single two-level atom. This set-up will be discussed in the following.

5. The one-atom maser

The Rydberg maser experiment [23] employs an atomic beam to ensure collision-free conditions for the highly excited Rydberg states. A diagram of the vacuum chamber with atomic beam arrangement and microwave cavity is shown in fig.4. These parts are mounted inside a helium bath cryostat. In the experiment, rubidium atoms with a Maxwellian velocity distribution are used. (The velocity selector is inserted at a later stage of the experiment). The atoms enter through small apertures into the liquid helium cooled part of the apparatus. There, the atoms are excited by laser radiation to the upper maser level and enter the cavity. Behind the cavity, they are monitored by field ionization and the subsequent detection of the ejected electrons in a channeltron electron multiplier.

The $63p_{3/2}$ Rydberg state of ^{85}Rb was excited using the narrowband ($\delta\nu$=2MHz) frequency doubled ultraviolet light of a continuous wave dye laser. The cavity was manufactured from niobium. The frequency could be tuned by squeezing the cavity. The temperature could be varied from 4.3 to 0.5K, corresponding to Q factors of $1.7 \cdot 10^7$ and $3 \cdot 10^{10}$, respectively. Single photons could therefore be stored up to 200ms. The thermal background field inside the cavity is determined by the temperature of the walls. The average number of photons of blackbody radiation per mode is $n=[\exp(h\nu/kT)-1]^{-1}$, which gives about n=3.8 at 4.3K and 0.15 at 0.5K (ν=21.5GHz). The continuous wave excitation requires also a continuous detection of the Rydberg atoms. Having left the cavity, the Rb atoms move into the inhomogeneous electric field of a plate capacitor. If the maximum field strength is chosen properly, atoms in the initially prepared $63p_{3/2}$ state are selectively ionized. Transitions to other levels are thus detected by a reduction of the electron count rate.

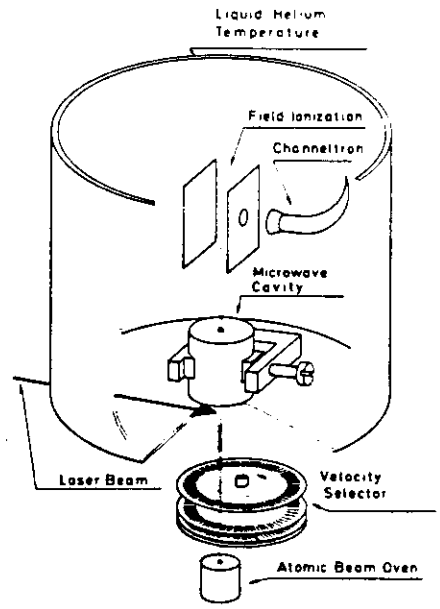

Fig.4: One-atom maser with atomic beam, velocity selector and microwave cavity. The upper part is cooled to liquid helium temperature.

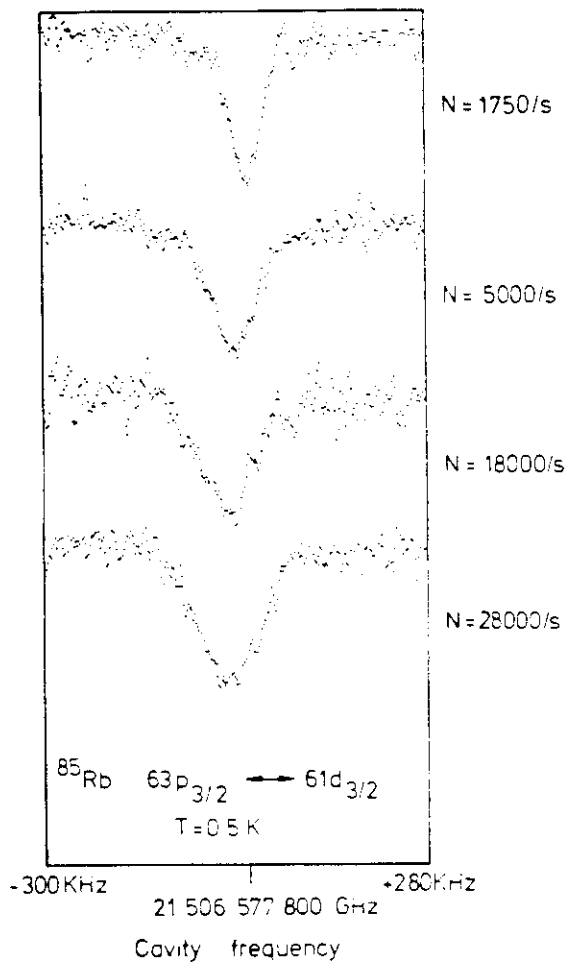

Fig.5: Maser resonances $63p_{3/2}$-$61d_{3/2}$ at a temperature of 0.5K.

To demonstrate maser operation, the cavity was tuned over the $63p_{3/2}$-$61d_{3/2}$ transition (see fig.5). An increase in flux caused power broadening and a small shift. This shift is attributed to the ac Stark effect caused predominantly by virtual transitions to the $61d_{5/2}$ level, which is only 50MHz away from the maser transition. The fact that the field ionization signal at resonance is independent of the particle flux indicates that the transition is saturated. Together with the observed power broadening, this shows that there is a multiple exchange of photons between Rydberg atoms and the cavity field.

With an average transit time of the Rydberg atoms through the cavity of 50μs, one calculates for a flux of 1750 atoms per second a probability of 0.09 of finding an atom in the cavity. According to Poisson statistics, this implies that more than 90 per cent of the events are due to a single atom. This clearly demonstrates that single atoms are able to maintain continuous oscillations of the cavity.

Since the transition is saturated, half of the atoms initially excited in the $63p_{3/2}$ state leave the cavity in the lower $61d_{3/2}$ maser

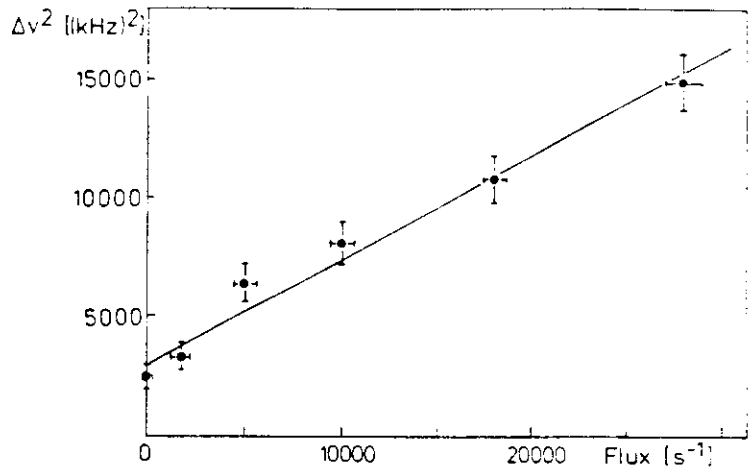

Fig.6: Squares of the halfwidth of the maser resonances versus atomic flux. The straight line shows that power broadening is present. This proves that a maser field is built up in the cavity.

level. For the average transit time of 50μs the decay to other levels can be neglected. The energy radiated by those atoms is stored in the cavity for its decay time, increasing the field strength. The average number of photons left in the cavity by the Rydberg atoms is given by

$$n_m = \tau_d(N/2)$$

where τ_d is the characteristic decay time of the cavity and N the number of Rydberg atoms entering the cavity in the upper maser level per unit time. For the highest particle flux used in our experiment $N=28\cdot10^3$ atoms per second, one finds n=400 Photons at 0.5K ($\tau_d\approx30$ms).

When the squares of the halfwidth $\delta\nu$ of the signal curves are plotted versus the Rydberg atom flux, a straight line is obtained as expected (fig.6). This line intersects the $(\delta\nu)^2$ axis at a finite value determined by transit time broadening.

The coupling constant between atom and radiation is large enough for a multiple exchange of photons between the cavity mode and a single Rydberg atom to occur. It follows that under the conditions of the experiment the atom performs on the average up to 3 Rabi periods during its passage through the cavity. Before discussing the experimental results of this Rabi-nutation, we review the main effects predicted by the Jaynes-Cummings model that describes the interaction of a single two-level atom with a single mode of the radiation field (see also [46-47]).

6. The Jaynes-Cummings model

For a brief discussion of the theoretical predictions of the Jaynes-Cummings model [25-34], we consider a two-level atom which enters a resonant cavity with a field of n photons. The time development of the probability $P_{e,n}$ of the atom in the excited state is then given by

$$P_{e,n}(t) = \cos^2(\Omega(n+1)^{1/2}t)$$

where Ω is the single-photon Rabi frequency, which can be determined from the dipol matrix element and the cavity mode structure.

In the realistic case, there will always be a fluctuating number of photons initially present in the cavity and the quantum Rabi solution has to be averaged over the probability distribution p(n) of having n photons in the mode at t = 0:

$$P_{e,n}(t) = \sum_{n=0}^{\infty} p(n) \cos^2(\Omega(n+1)^{1/2}t)$$

At a low atomic beam flux, the cavity contains essentially thermal photons and their number is a random quantity conforming to Bose-Einstein statistics. In this case, p(n) is given by

$$p_{th}(n) = n_{th}^{n}/(n_{th} + 1)^{n+1},$$

with the average number of thermal photons $n_{th}=[\exp(h\nu/kT)-1]^{-1}$. The distribution of Rabi frequencies then results in an apparent random oscillation $P_{e,th}$.

At higher atomic beam fluxes, the number of photons produced by stimulated emission in the cavity will increase and the statistics change. For a Poissonian distribution representing a coherent field:

$$p_c(n) = \exp(-\langle n\rangle)\cdot\langle n\rangle^{n}/n!$$

As first shown by Cummings, the Poisson spread in n gives dephasing of the Rabi oscillations, therefore $P_{e,c}$ first exhibits a collapse [26]. This is described in the resonant case by the approximate envelope $\exp(-\Omega^2t^2/2)$ and is independent of the average photon number $\langle n\rangle$ [30]. After the collapse, there is a range of interaction times for which $P_{e,c}$ is independent of time, and this even in the absence of a decay mechanism in the model [26-34]. Later, $P_{e,c}$ exhibits recorrelations (revivals) and starts oscillating again in a complex way. As has been shown by Eberly and co-workers, the recurrences occur at times given by [30]

$$t = kT_R \quad (k = 1,2,3,\ldots), \qquad \text{with } \Omega T_R = 2\pi n^{1/2}$$

The revival in the coherent field is a pure quantum feature and has no classical counterpart. Eberly and co-workers have shown that the physical reason for collapse and revival is the Poisson photon number distribution leading to a "granularity" of the quantized radiation field present even at high average photon numbers.

This can be understood by noting that only a classical field can have a well defined amplitude and phase. However, in quantum mechanics, Heisenberg's uncertainty relation imposes an upper limit on the product of the variances of two canonically conjugate variables like the number of photons and the phase of the field. The minimum uncertainty state of the radiation field corresponds to a Poissonian number distribution. This represents a coherent wave in the classical limit. In this case, the phenomena of collapse and revival of the Rabi-nutation are observed.

The inversion also collapses and revives in the case of a chaotic Bose-Einstein field [33]. Here, the photon number spread is larger than for a coherent state. As a consequence the collapse time is much shorter. In addition, the revivals completely overlap and interfere to produce a very irregular time evolution. A classical thermal field represented by a Gaussian distribution of amplitudes also shows collapse, but revivals are absent. Therefore, the revival can be considered as a clear quantum feature, but the collapse is less clear-cut as a quantum effect.

We conclude this section by noting that in the case of Raman type two photon processes the Rabi frequency turns out to be $2\Omega n$ rather than $2\Omega(n+1)^{1/2}$, enabling the sum over the photon numbers in $P_{e,c}$ to be carried out in simple closed form. In this case, the inversion revives perfectly with a completely periodic sequence [34].

7. Single atom inside a resonant cavity - oscillatory regime

The experimental set-up described in section 5 is suitable to test the Jaynes-Cummings model. An important requirement is that the atoms of the beam have a homogeneous velocity so that it is possible to observe the Rabi-nutation induced by the cavity field directly. This is not possible with the broad Maxwellian velocity distribution. A Fizeau-type velocity selector is therefore inserted between the atomic beam oven and the cavity, so that a fixed atom-field interaction time is obtained [24]. Changing the selected velocity leads to a different interaction time and leaves the atom in another phase of the Rabi cycle when it reaches the detector.

The experimental results obtained for the $63p_{3/2}$-$61d_{5/2}$ transition are shown in fig. 7-9. In the figures the ratio between the field ionization signals on and off resonance are plotted versus the interaction time of the atoms in the cavity. The solid curve in fig.7 was calculated using the Jaynes-Cummings model, which is in very good agreement with the experiment. The total uncertainty in the velocity of the atoms is 4% in this measurement. The error in the signal follows from the statistics of the ionization signal and amounts to 4%. The measurement is made with the cavity at 2.5K and $Q=2.7\cdot10^8$ ($\tau_d=2$ms). There are on the average 2 thermal photons in the cavity. The number of maser photons is small compared with the number of blackbody photons.

The experimental result shown in fig. 7 is obtained with very low atomic beam flux ($N = 500s^{-1}$ and $n_m = 0.5$; n_m is the number of photons accumulated in the cavity). When the atomic beam flux is increased, more photons are piled up in the cavity. Measurements with $N = 2000s^{-1}$ ($n_m = 2$) and $N = 3000s^{-1}$ ($n_m = 3$) are shown in figs. 8 and 9. The maximum of $P_e(t)$ at 70μs flattens with increasing photon number, thus demonstrating the collaps of the Rabi nutation induced by the resonant maser field. Figs. 8 and 9 together show that for atom-field interaction times between 50μs and about 130μs $P_e(t)$ does not change as a function of time. Nevertheless, at about 150μs, $P_e(t)$ starts to oscillate again (fig. 9), thus showing the revival predicted by the Jaynes-Cummings model. The variation of the Rabi nutation dynamics with increasing atomic beam fluxes and thus with increasing photon numbers in the cavity generated by stimulated emission is obvious from figs. 7-9.

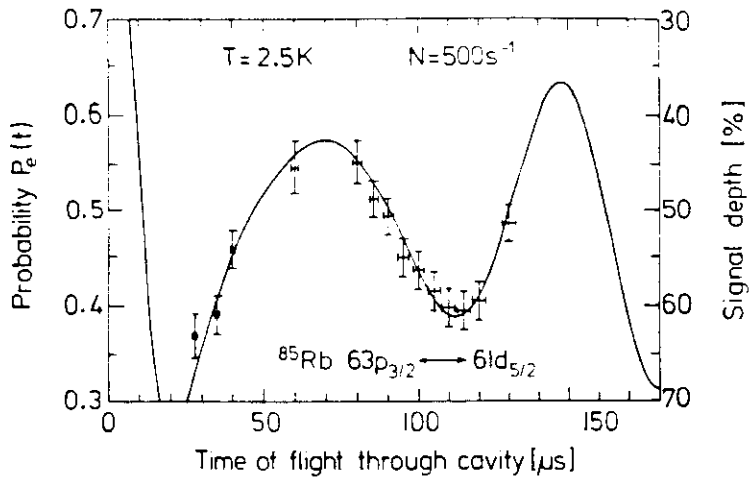

Fig.7: Measured probability of finding the atom in the upper maser level with the cavity tuned to the $63p_{3/2}$-$61d_{5/2}$ transition. The flux of Rydberg atoms is $N=500s^{-1}$. The solid line represents the theoretical prediction.

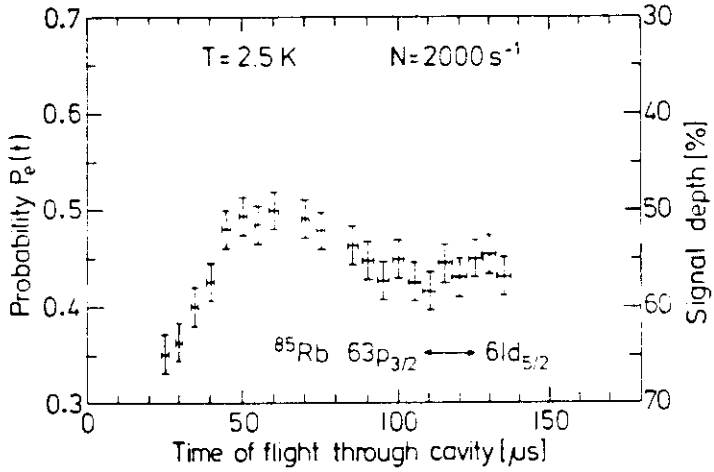

Fig.8: Same as fig. 7, but the flux of Rydberg atoms is $N=2000s^{-1}$.

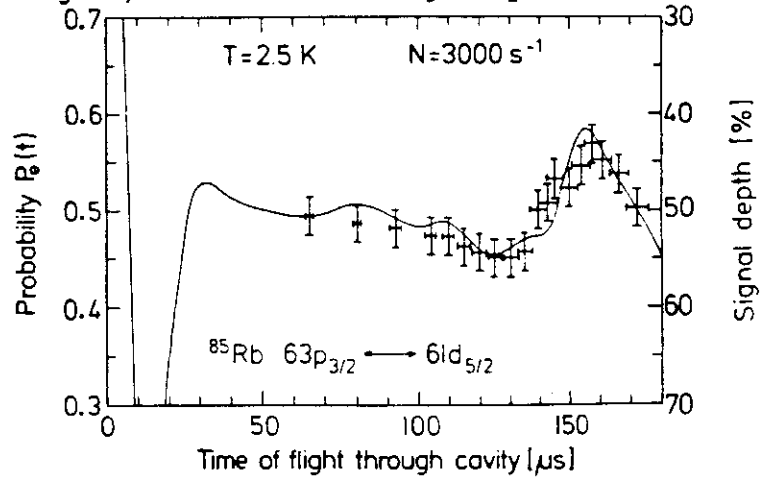

Fig.9: Same as fig. 7, but the flux of Rydberg atoms is $N=3000s^{-1}$.

8. Maser radiation below the shot noise limit

The results discussed in section 7 represent the change of the Rabi-nutation with increasing flux of atoms. This means that the photon statistics also change starting with a Bose-Einstein distribution. Now we will discuss the photon statistics in the maser cavity, which under appropriate conditions turn out to be nonclassical [35-40]. The maser field therefore has to be described within the framework of quantum mechanics.

There are two approaches to the quantum theory of the one-atom maser. Filipowicz et al. [35] describe the device via a microscopic approach. On the other hand, Lugiato et al. [36] show that the standard macroscopic quantum laser theory leads to the same steady state photon statistics. The special features of the one atom maser were not emphasized in the standard laser theory because the broadening due to spontaneous decay obscured the Rabi cycling of the atoms [48]. When similar averages in the microscopic theory associated with inhomogeneous (interaction time) broadening are performed, equivalent results are obtained.

In the one-atom maser, the photon statistics depend on the normalized interaction time $\theta = \Omega t(\tau_d/t_a)^{1/2}$, where t is the interaction time of the atoms and the field, τ_d the photon damping time of the cavity, and t_a the average time between two atoms entering the cavity after each other. At threshold $\theta=1$, the photon statistics are first strongly super-Poissonian (i.e. $\sigma^2=(\langle n^2\rangle-\langle n\rangle^2)/\langle n\rangle \gg 1$). There are further super-Poissonian regions around $\theta \approx 2\pi k$ ($k=1,2,\ldots$). These peaks become less pronounced for increasing θ. Between these peaks, the field becomes sub-Poissonian. Since the experimental results are in good agreement with the Jaynes-Cummings theory it can also be expected that the photon statistics of the micromaser field is sub-Poissonian for most interaction times θ.

For a cavity with a quality factor of $Q=3\cdot10^{10}$, the lifetime of the photons in the resonator amounts to 200ms. This time is then long compared to the buildup time of the micromaser field; furthermore, no thermal field is present anymore since the cavity is operated at temperatures lower than 0.5K. Under these circumstances, fluctuations are suppressed in the experiment and it is possible to obtain a pure number state of the field in the cavity [37-38]. The Rydberg atoms which were injected into the cavity in the upper state are probed for excitation when they leave the cavity. When all the atoms are counted which are in the lower state (and which therefore have emitted a photon), the total number of photons in the cavity is known, assuming that there were no photons in the cavity at the beginning of the experiment.

This means that the state of the field is reduced to a pure number state by the determination of the number of atoms that have emitted a photon. The photon number of the field is always fixed and known after the experiment. Before the experiment starts, however, only the probability to obtain a certain photon number n is known, depending on the number of interacting atoms m. This probability distribution must not be confused with the photon statistics of the maser field. In this case, the photon number distribution of the field is always a δ-function. Therefore, the one-atom maser is a new tool for studying the influence of repeated measurements on a single quantum system. New dynamics and instabilities are expected [49] which are not apparent when conventional

ensemble average predictions are considered. Experiments to measure the highly nonclassical maser field have just been completed in our laboratory and will be presented elsewhere [50].

9. Conclusion

We have reviewed progress towards developing Rydberg atoms as tools to test basic principles of quantum electrodynamics. Their unique properties lead to a situation where it is for the first time possible to study light-matter interaction in confined space such as: switching-off the vacuum, enhancing spontaneous emission, modifying the Lamb shift and testing the Jaynes-Cummings model. Further areas of investigation not mentioned here, such as the classical/quantum chaos [51-53], present further evidence for the increasing importance of Rydberg atoms in fundamental research. In addition, the one-atom maser can be used as a new probe of complementarity in quantum mechanics [54]. Rydberg atoms were also used to demonstrate for the first time maser operation on a two-photon transition [55]. The tremendous experimental progress of the last years also promises exciting and surprising results for the future.

References

[1] Stebbings, R.F., and Dunning, F.B., (ed.), Rydberg States of Atoms and Molecules, (Cambridge University Press).
[2] Gallagher, T.F., and Cooke, W.E., 1979, Phys. Rev. Lett., **42**,835.
[3] Haroche,S., Fabre,C., Goy,M., Gross,M. and Raimond,J., 1979, Laser Spectroscopy IV, ed. H. Walther, and K.W. Rothe, (Berlin: Springer)
[4] Beiting, E.J., Hildebrandt, G.F., Kellert, F.G., Foltz, G.W., Smith K.A.,Dunning, F.B., and Stebbings, R.F., 1979, J.Chem.Phys.,**70**,3351
[5] Koch, P.R., Hieronymus, H., Van Raan, F.J., and Raith, W., 1980, Phys. Lett. A **75**,273.
[6] Rempe, G., 1981, Thesis, University of Munich (unpublished).
[7] Figger, H., Leuchs, G., Straubinger, R., and Walther, H., 1980, Optics Commun., **33**,37.
[8] Rempe, G., 1986, Thesis, University of Munich (unpublished).
[9] Purcell, E.M., 1946, Phys. Rev., **69**,681.
[10] Drexhage, K.H., 1974, Progress in Optics, Vol. 12, ed. E. Wolf (Amsterdam: North-Holland), p. 165.
[11] Milonni, P.W., and Knight, P.L., 1973, Opt. Commun. **9**,119.
[12] Kleppner, D., 1981, Phys. Rev. Lett., **47**,233.
[13] Gabrielse, G., and Dehmelt, H., 1985, Phys. Rev. Lett., **55**,67.
[14] Vaidyanathan, A., Spencer, W., and Kleppner, D., 1981, Phys. Rev. Lett., **47**,1592.
[15] Hulet,R.G., Hilfer,E.S., Kleppner,D., 1985, Phys.Rev.Lett. **55**,2137
[16] Jhe, W., Anderson, A., Hinds, E.A., Meschede, D., Moi, L., Haroche, S., 1987, Phys. Rev. Lett. **58**,666
[17] Heinzen,D.J., Childs,J.J., Thomas,J.F., Feld,M.S., 1987, Phys. Rev. Lett **58**,1320. Heinzen,D.J., Feld,M.S., 1987, Phys.Rev.Lett. **59**,2623
[18] DeMartini, F., Innocenti, G., Jacobovitz, G.R., Mataloni, P., 1987, Phys. Rev. Lett. **59**,2955
[19] Goy, P., Raimond, J.D., Gross, M., and Haroche, S., 1983, Phys.

Rev. Lett., **50**,1903.
[20] Dobiasch, P., and Walther, H., 1985, Ann. Phys. Fr. **10**,825.
[21] Lütken, C.A., and Ravndal, F., 1985, Phys. Rev. A **31**,2082.
[22] Barton, G., 1987, Proc. R. Soc. London, A**410**,141 and 175.
[23] Meschede,D., Walther,H., and Müller,G., 1985, Phys.Rev.Lett.,**54**,551
[24] Rempe, G., Walther, H., and Klein, N., 1987, Phys.Rev.Lett. **58**,353.
[25] Jaynes, E.T., and Cummings, F.W., 1963, Proc. IEEE, **51**,89.
[26] Cummings, F.W., 1965, Phys. Rev. A, **140**,1051.
[27] Stenholm, S., 1973, Phys. Rep., **6**,1.
[28] Von Foerster, T., 1975, J. Phys. A, **8**,95.
[29] Meystre, P., Geneux, E., Quattropani, A., and Faist, A., 1975, Nuovo Cim. B**25**,521.
[30] Eberly, J.H., Narozhny, N.B., and Sanchez-Mondragon, J.J., 1980, Phys. Rev. Lett., **44**,1323.
[31] Knight, P.L., and Milonni, P.W., 1980, Phys. Rep., **66**,21.
[32] Yoo, H.-I., and Eberly, J.H., 1985, Phys. Rep. **118**,239.
[33] Knight, P.L., and Radmore, P.M., 1982, Phys. Lett. **90A**,342.
[34] Knight, P.L., 1986, Physica Scripta, T**12**,51.
[35] Filipowicz, P., Javanainen, J., and Meystre, P., 1986, Phys. Rev. A **34**,3077.
[36] Lugiato,L.A., Scully,M.O., and Walther,H., 1987, Phys.Rev. A **36**,740
[37] Filipowicz, P., Javanainen, J., and Meystre, P., 1986, J. Opt. Soc. Am. B **3**,906
[38] Krause, J., Scully, M.O., and Walther, H., 1987, Phys.Rev.A **36**,4547
[39] Krause, J., Scully, M.O., Walther, T., and Walther, H., 1989, Phys. Rev. A **39**,1915.
[40] Meystre, P., Rempe, G., and Walther, H., 1988, Opt. Lett., **13**,1078.
[41] Farley, J.W., and Wing, W.H., 1981, Phys. Rev. A **23**,2397.
[42] Hollberg, L., and Hall, J.L., 1984, Phys. Rev. Lett. **53**,230.
[43] Gallagher, T.F., Sandner, W., Safinya, K.A., and Cook, W.E., 1981, Phys. Rev. A **23**,2065.
[44] Weisskopf, V., and Wigner, E., 1930, Z. Phys., **63**,54.
[45] Bloembergen, N., and Pound, R.V., 1954, Phys. Rev., **95**,8.
[46] Haroche, S., and Raimond, J.M., 1985, Advances in Atomic and Molecular Physics, Vol. 20, ed. B. Bates and B. Bederson (New York: Academic Press), p. 347.
[47] Gallas, J.A.C., Leuchs, G., Walther, H., and Figger, H., 1984, Advances in Atomic and Molecular Physics, Vol. 20, ed. B. Bates and B. Bederson (New York: Academic Press), p. 412.
[48] Sargent, M., Scully, M.O., and Lamb Jr., W.E., 1974, Laser Physics, (Reading: Addison Wesley).
[49] Meystre, P., and Wright, E.M., 1988, Phys. Rev. A **37**,2524
[50] Rempe, G., Schmidt-Kaler, F., and Walther, H., to be published
[51] Casati, G., Chirikov, B.V., and Shepelyanski, D.L., 1984, Phys. Rev. Lett., **53**,2525.
[52] Bayfield, J.E., and Pinnaduwage, L.A., 1985, Phys.Rev.Lett., **54**,313
[53] Blümel, R., Graham, R., Sirko, L., Smilanski, U., Walther, H., and Yamada, K., 1989, Phys. Rev. Lett. **62**,341.
[54] Scully, M.O., and Walther, H., 1989, Phys. Rev. A **39**,5229.
[55] Brune, M., Raimond, J.M., Goy, P., Davidovich, L., and Haroche, S., 1987, Phys. Rev. Lett., **59**,1899.